Supporting figures for

Comprehensive evaluations of diurnal NO_2 measurements during DISCOVER-AQ 2011: Effects of resolution dependent representation of NO_x emissions

Jianfeng Li[1, a], Yuhang Wang[1*], Ruixiong Zhang[1], Charles Smeltzer[1], Andrew Weinheimer[2], Jay Herman[3], K. Folkert Boersma[4, 5], Edward A. Celarier[6, 7, b], Russell W. Long[8], James J. Szykman[8], Ruben Delgado[3], Anne M. Thompson[6], Travis N. Knepp[9, 10], Lok N Lamsal[6], Scott J Janz[6], Matthew G Kowalewski[6], Xiong Liu[11], Caroline R. Nowlan[11]

[1]School of Earth and Atmospheric Sciences, Georgia Institute of Technology, Atlanta, Georgia, USA
[2]National Center for Atmospheric Research, Boulder, Colorado, USA
[3]University of Maryland Baltimore County JCET, Baltimore, Maryland, USA
[4]Royal Netherlands Meteorological Institute, De Bilt, the Netherlands
[5]Wageningen University, Meteorology and Air Quality Group, Wageningen, the Netherlands
[6]NASA Goddard Space Flight Center, Greenbelt, Maryland, USA
[7]Universities Space Research Association, Columbia, Maryland, USA
[8]National Exposure Research Laboratory, Office of Research and Development, U.S. Environmental Protection Agency, Research Triangle Park, NC, USA
[9]NASA Langley Research Center, Virginia, USA
[10]Science Systems and Applications, Inc., Hampton, Virginia, USA
[11]Harvard-Smithsonian Center for Astrophysics, Cambridge, Massachusetts, USA

[a]now at: Atmospheric Sciences and Global Change Division, Pacific Northwest National Laboratory, Richland, Washington, USA
[b]now at: Digital Spec, Tyson's Corner, VA, USA

[*] *Correspondence to* Yuhang Wang (yuhang.wang@eas.gatech.edu)

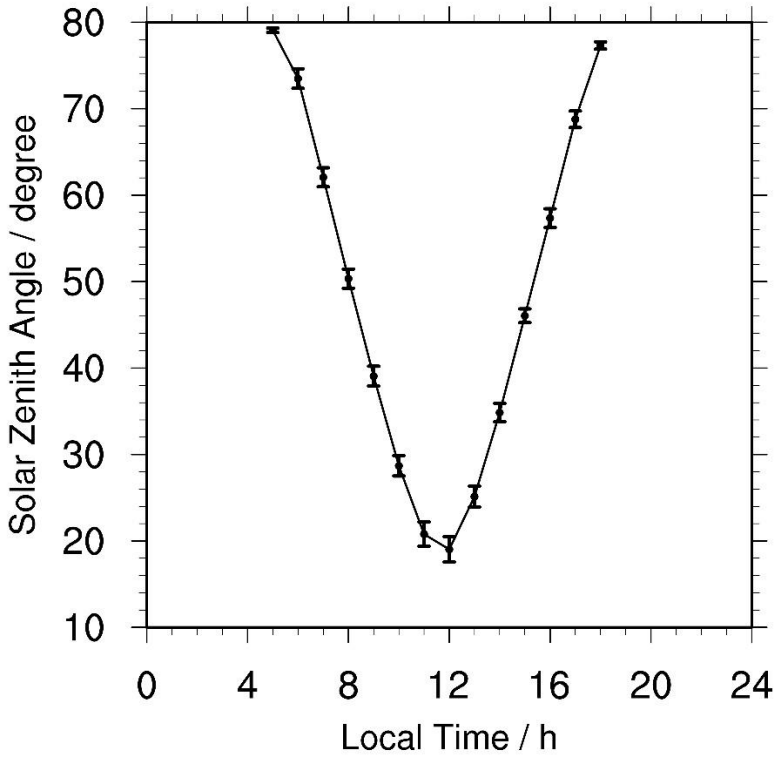

Figure S1. Diurnal variations of the solar zenith angles of Pandora measurements in July 2011. Here we use monthly averages of the 11 inland Pandora sites (Table S1 and Figure 1). Error bars denote standard deviations.

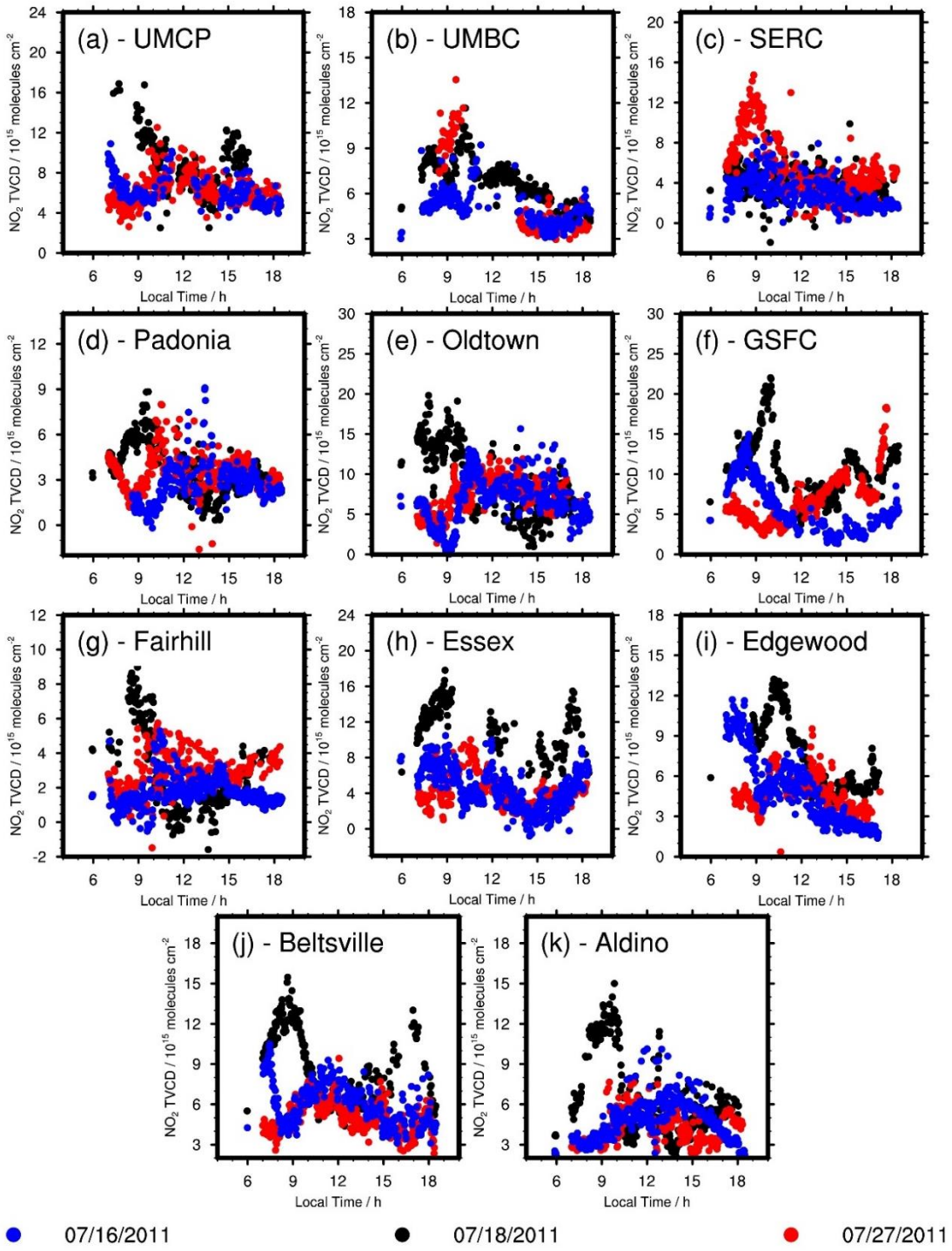

Figure S2. Daily variations of Pandora NO_2 TVCDs at the 11 inland sites for three randomly selected days in July 2011. Blue dots denote Pandora measurements on July 16, 2011 (Saturday), black dots denote July 18, 2011 (Monday), and red dots denote July 27, 2011 (Wednesday). Here Pandora NO_2 TVCDs are calculated by subtracting stratospheric NO_2 VCDs from Pandora total NO_2 VCDs. See the main text for details.

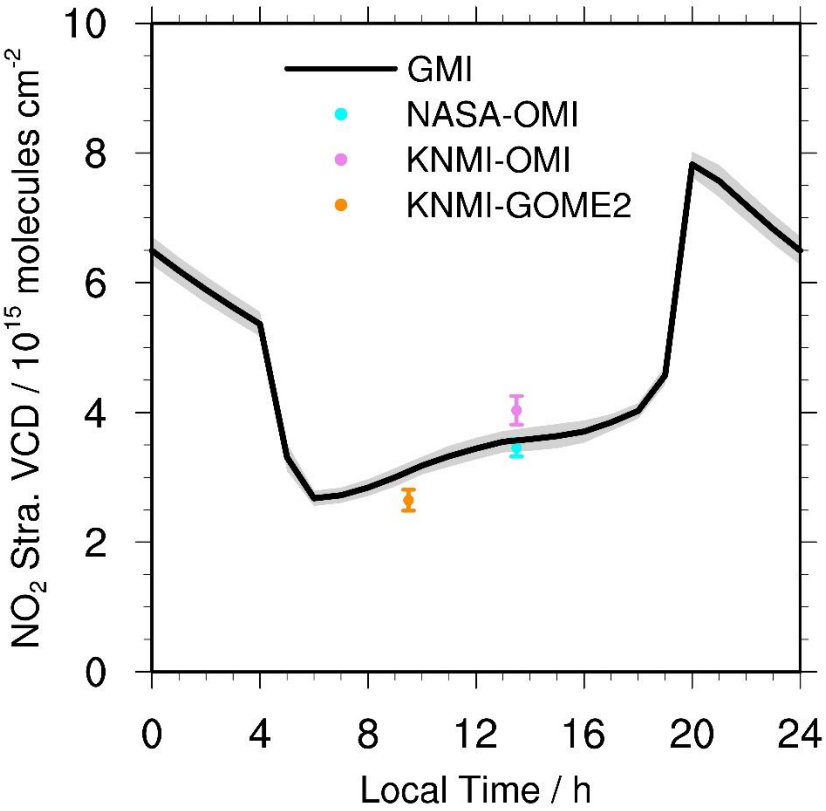

Figure S3. Stratospheric NO_2 VCD diurnal variations at the Greenbelt station in Maryland (39° N, 76.89° W) from the GMI MERRA-2 1° × 1.25° simulation (https://gmi.gsfc.nasa.gov/merra2hindcast/, last access: May 14, 2019) for July 2011, and the corresponding satellite stratospheric NO_2 VCDs in the DISCOVER-AQ region (about 39.2° N, 76.3° W) (Figure 1). "NASA-OMI" denotes the OMI NO_2 VCDs from NASA, "KNMI-OMI" denotes the OMI NO_2 VCDs from KNMI, and "KNMI-GOME2" denotes the GOME-2A NO_2 VCDs from KNMI. Gray shading and vertical bars denote the standard deviations of the GMI results and satellite stratospheric VCD products, respectively.

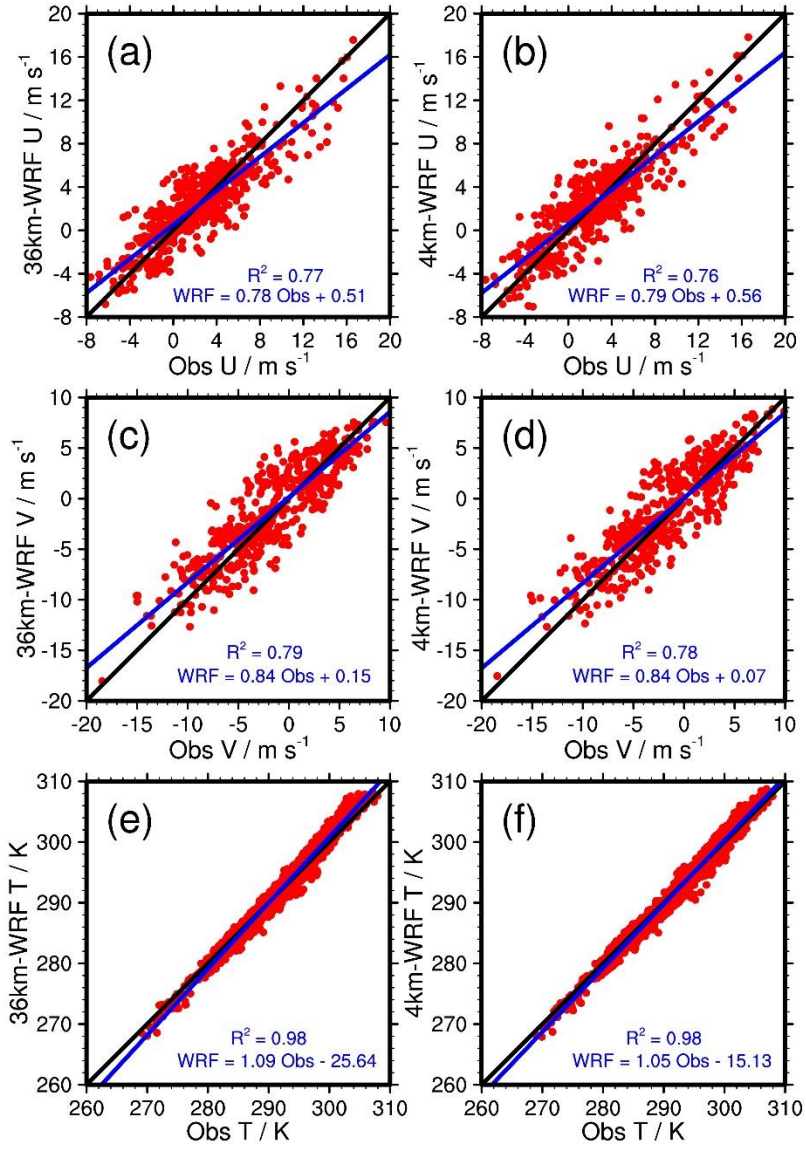

Figure S4. Comparisons of (a, b) U wind, (c, d) V wind, and (e, f) temperature (T) between P-3B spirals and coincident WRF simulation results for July 2011. For the P-3B observations, we derive U and V wind from the observed wind speed and wind direction (Figure S5), which were measured via a Honeywell INS sensor. The accuracies of P-3B wind speed and wind direction are 1 m s^{-1} and ± 5°, respectively. Air temperature on P-3B was measured by using a Rosemount model 102 sensor with an accuracy of ± 0.2 °C. The left panel is for comparisons between P-3B and the 36-km WRF simulation, and the right panel is for comparisons between P-3B and the nested 4-km WRF simulation. WRF wind components have been rotated to earth coordinates.

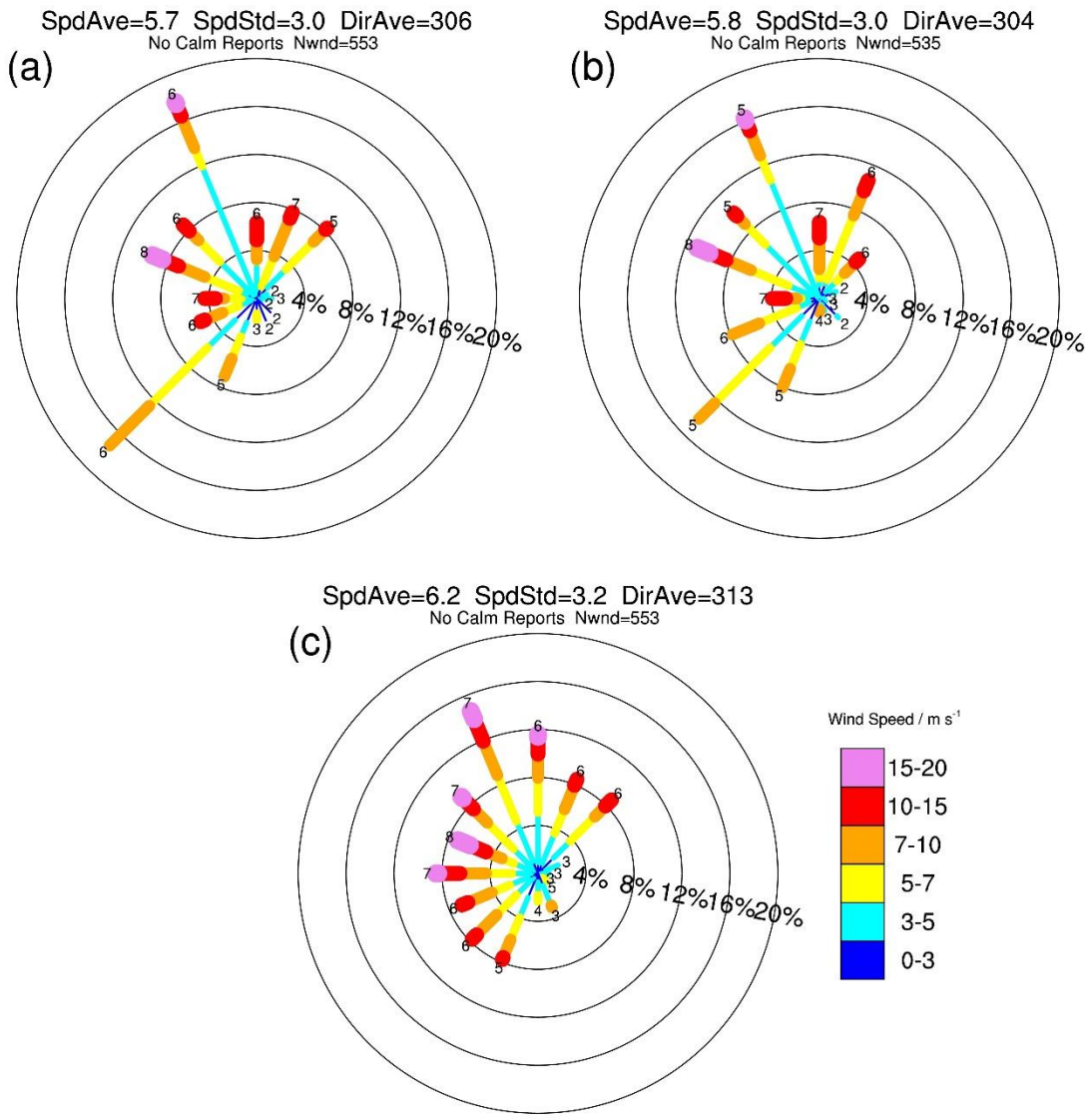

Figure S5. Wind roses for P-3B observations and coincident WRF simulation results for July 2011, (a) for the 36-km WRF simulation, (b) for the nested 4-km WRF simulation, and (c) for P-3B observations. WRF wind components have been rotated to earth coordinates. "SpdAve" denotes the average of wind speed, "SpdStd" denotes the standard deviation of wind speed, and "DirAve" denotes wind direction derived from averaged U-wind and V-wind.

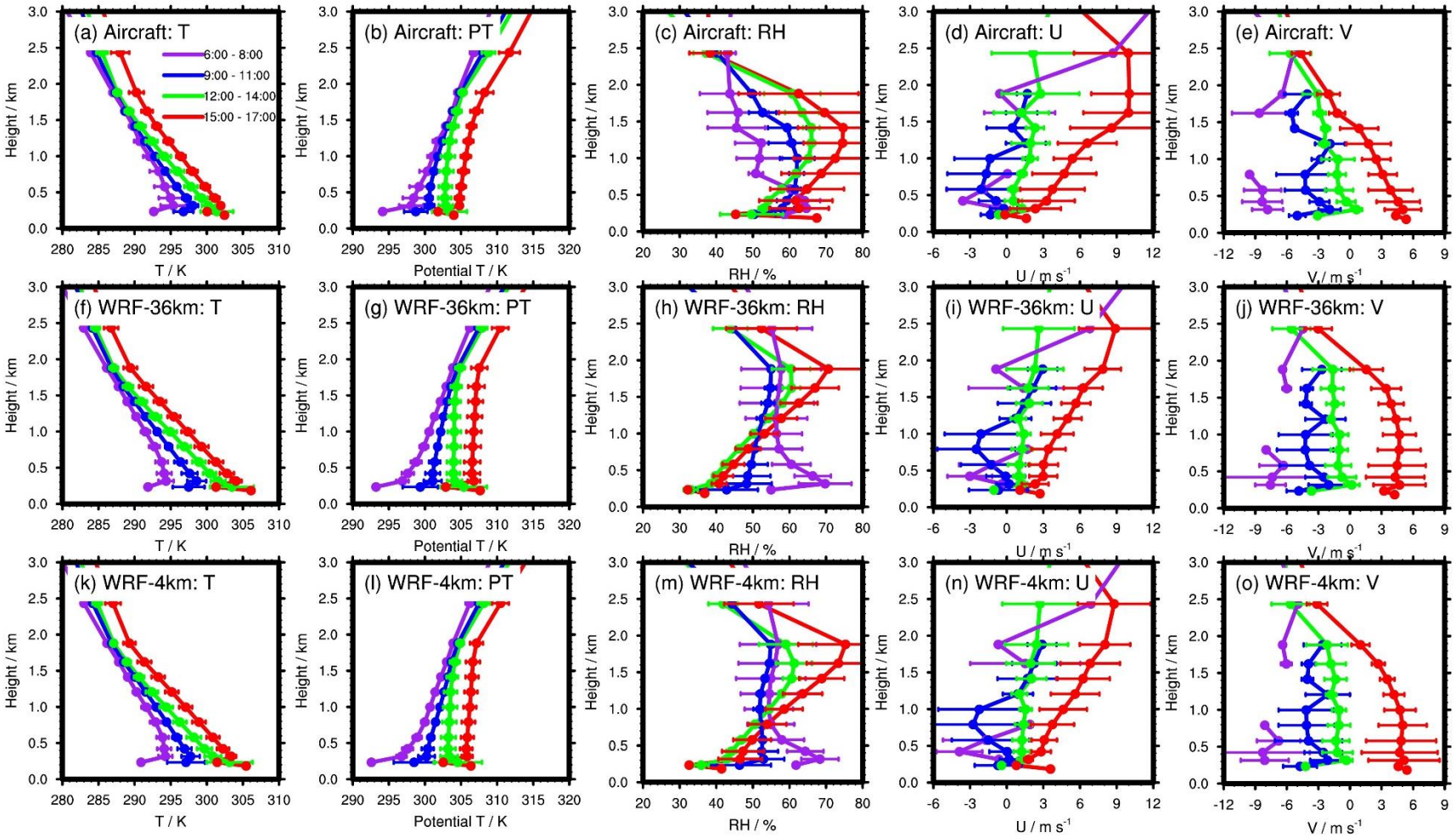

Figure S6. Temporal evolutions of vertical profiles for (a, f, k) temperature (T), (b, g, l) potential temperature (PT), (c, h, m) relative humidity (RH), (d, i, n) U-wind, and (e, j, o) V-wind below 3 km from the (a, b, c, d, e) P-3B aircraft and (f, g, h, i, j) 36-km and (k, l, ,m, n, o) nested 4-km WRF simulations during the DISCOVER-AQ campaign. Horizontal bars denote corresponding standard deviations. Purple lines denote 6:00 – 8:00 LT, blue lines for 9:00 – 11:00 LT, green lines for 12:00 – 14:00 LT, and red lines for 15:00 – 17:00 LT.

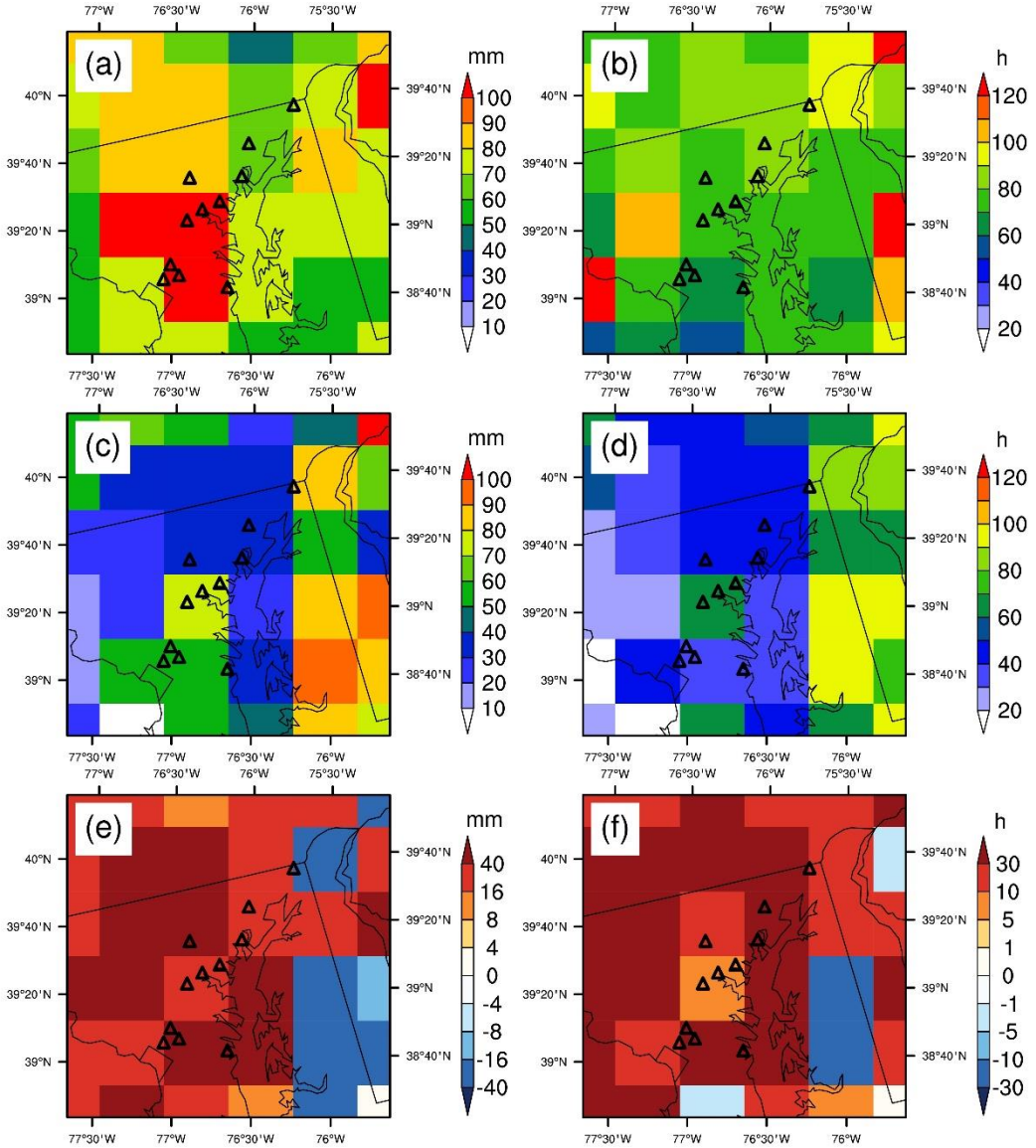

Figure S7. Distributions of (a, c) precipitation amounts and (b, d) precipitation durations in July 2011 for (a, b) Stage IV and (c, d) the 36-km WRF simulation. (e) and (f) are the differences in precipitation amount and precipitation duration between Stage IV and the 36-km WRF simulation. The original resolution of Stage IV is about 4 km over polar stereographic grids, and we regrid the dataset to the 36-km WRF pixels. Triangles denote the inland Pandora sites in Figure 1.

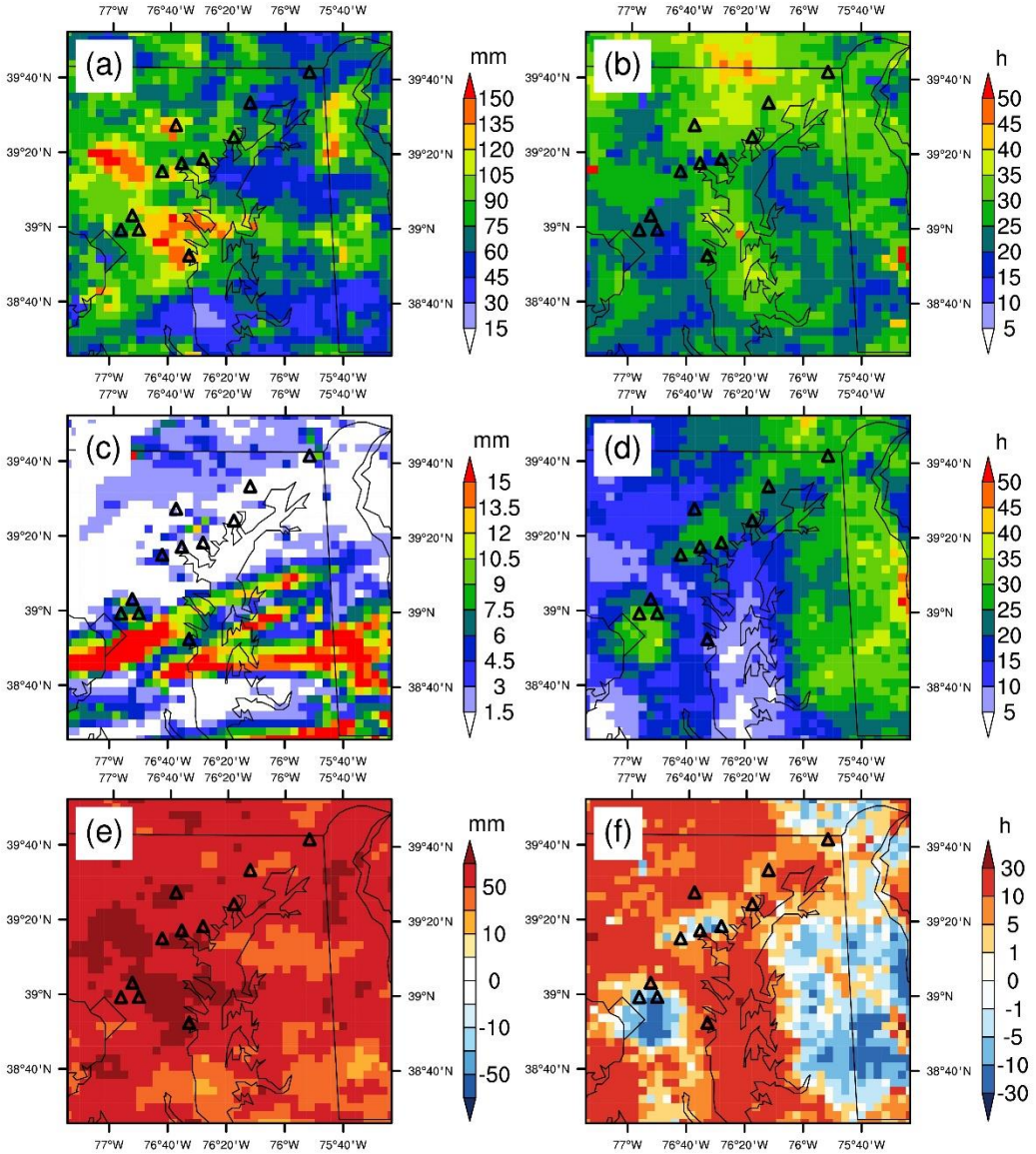

Figure S8. Distributions of (a, c) precipitation amounts and (b, d) precipitation durations in July 2011 for (a, b) Stage IV and (c, d) the nested 4-km WRF simulation. (e) and (f) stand for the differences in precipitation amount and precipitation duration between Stage IV and the nested 4-km WRF simulation. The original resolution of Stage IV is about 4 km over polar stereographic grids, and we regrid the dataset to the nested 4-km WRF pixels. Due to significantly lower precipitation amounts in the nested 4-km WRF simulation, we use different color bars for WRF and Stage IV data. Triangles denote the inland Pandora sites in Figure 1.

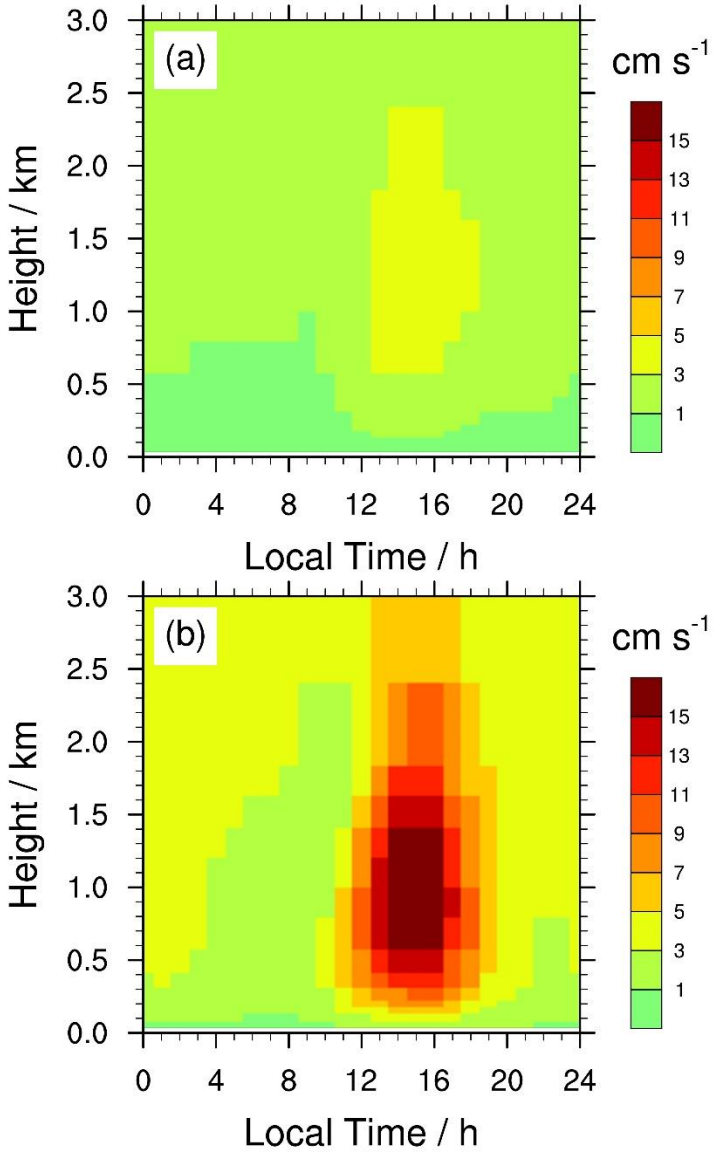

Figure S9. Diurnal variations of boundary-layer vertical velocities for the (a) 36-km and (b) nested 4-km WRF simulations in the DISCOVER-AQ region (Figure 1) for July 2011.

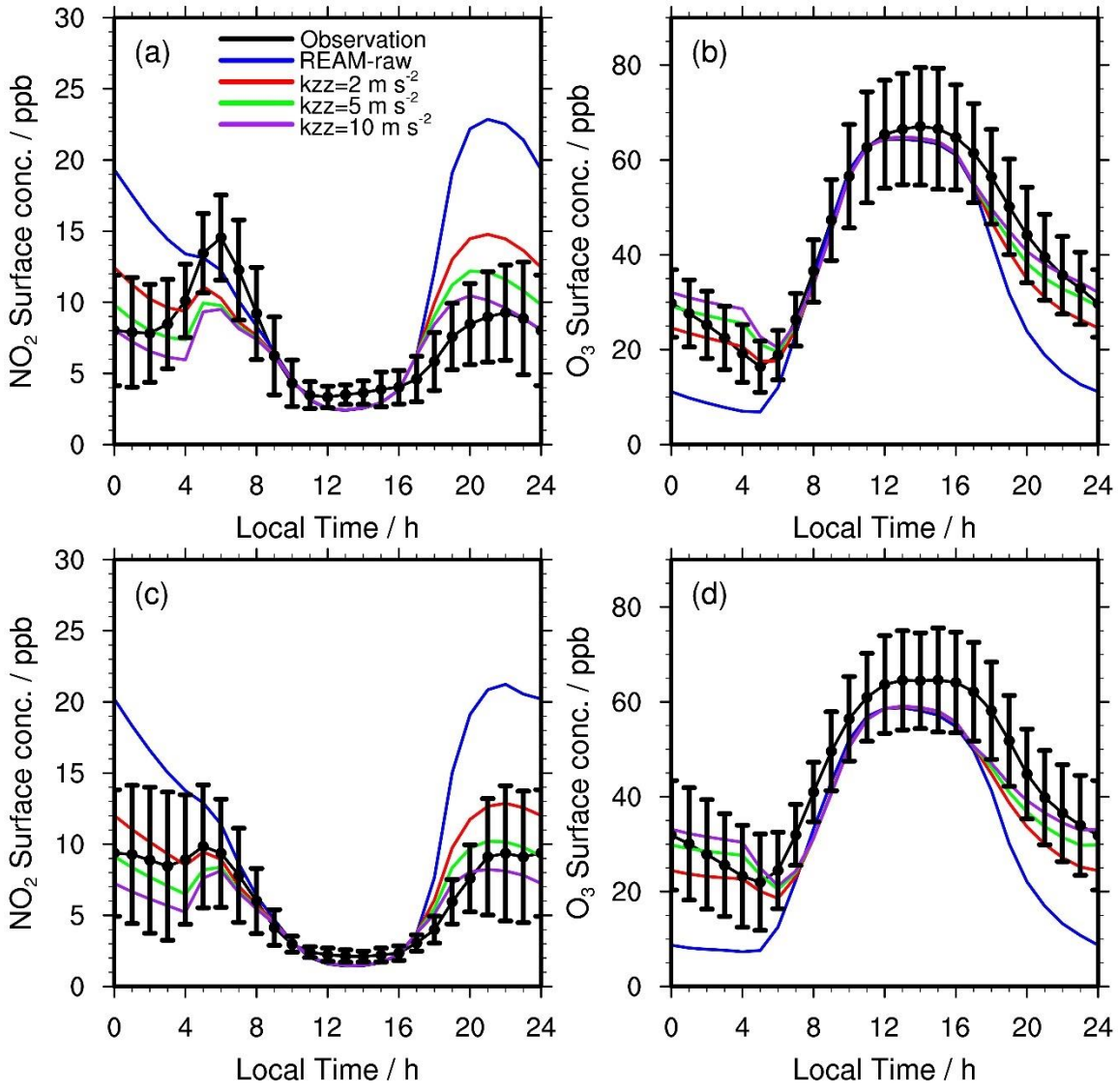

Figure S10. Similar as Figure 5 but with two additional REAM sensitivity tests with k_{zz} updated to 2 m s^{-2} or 10 m s^{-2} instead of 5 m s^{-2} following the approach mentioned in the main text.

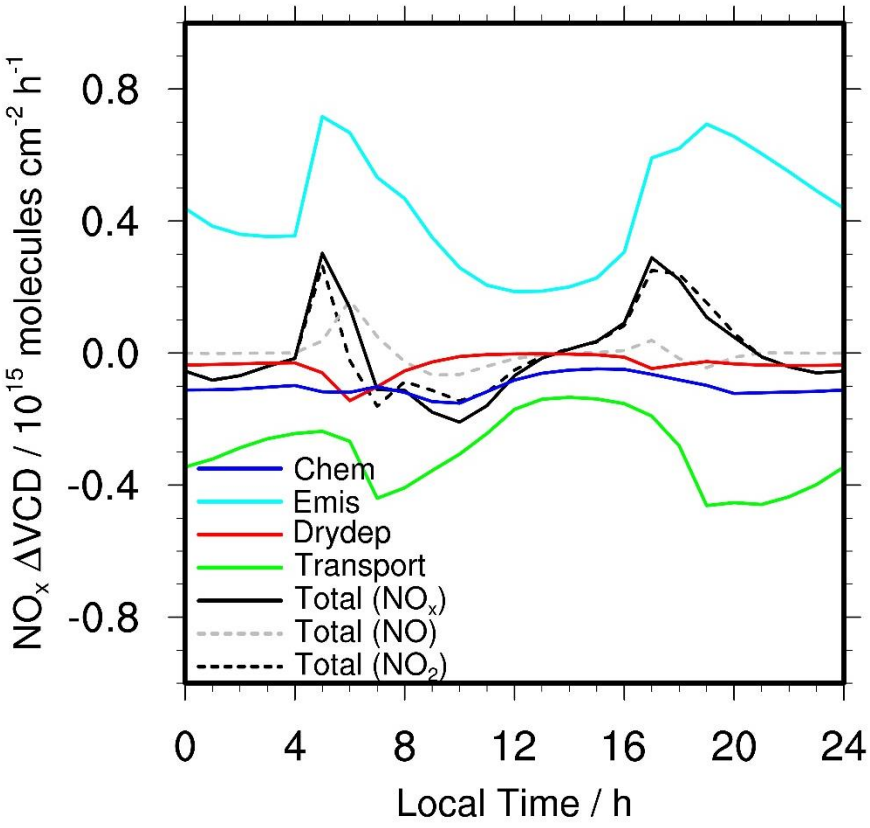

Figure S11. Contributions of emission, chemistry, transport, and dry deposition to NO_x VCD diurnal variations in the surface layer of the 36-km REAM simulation in the DISCOVER-AQ region on weekdays in July 2011. "Chem" refers to net NO_x chemistry production in the surface layer; "Emis" refers to NO_x emissions in the surface layer with the impact of vertical turbulent mixing; "Drydep" denotes NO_x dry depositions in the surface layer; "Transport" includes advection, turbulent mixing, lightning NO_x production, and wet deposition in the surface layer. "Total (NO_x)" is the hourly change of surface-layer NO_x VCDs ($\triangle(VCD) = VCD_{t+1} - VCD_t$). "Total ($NO_2$)" is the hourly change of surface-layer NO_2 VCDs, and "Total (NO)" is the hourly change of surface-layer NO VCDs.

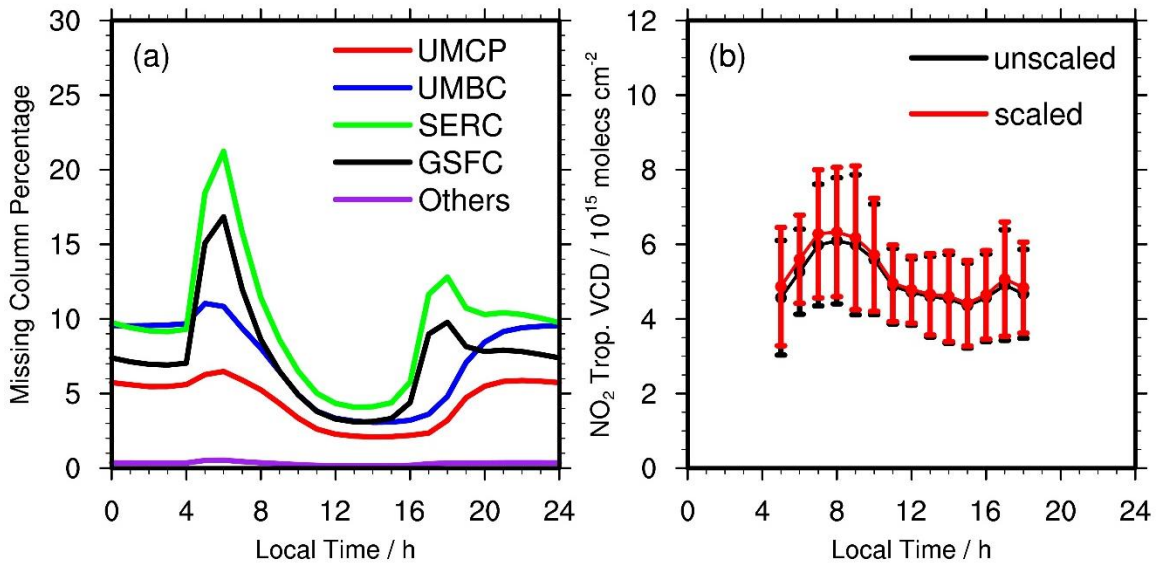

Figure S12. (a) Percentages of NO_2 VCDs below the heights of Pandora instruments in July 2011 based on 36-km REAM results; (b) the comparison between original Pandora TVCDs ("unscaled") and updated Pandora TVCDs ("scaled") with the inclusion of VCDs below the Pandora instruments. Here we use monthly averages in July 2011. Error bars in (b) denote standard deviations.

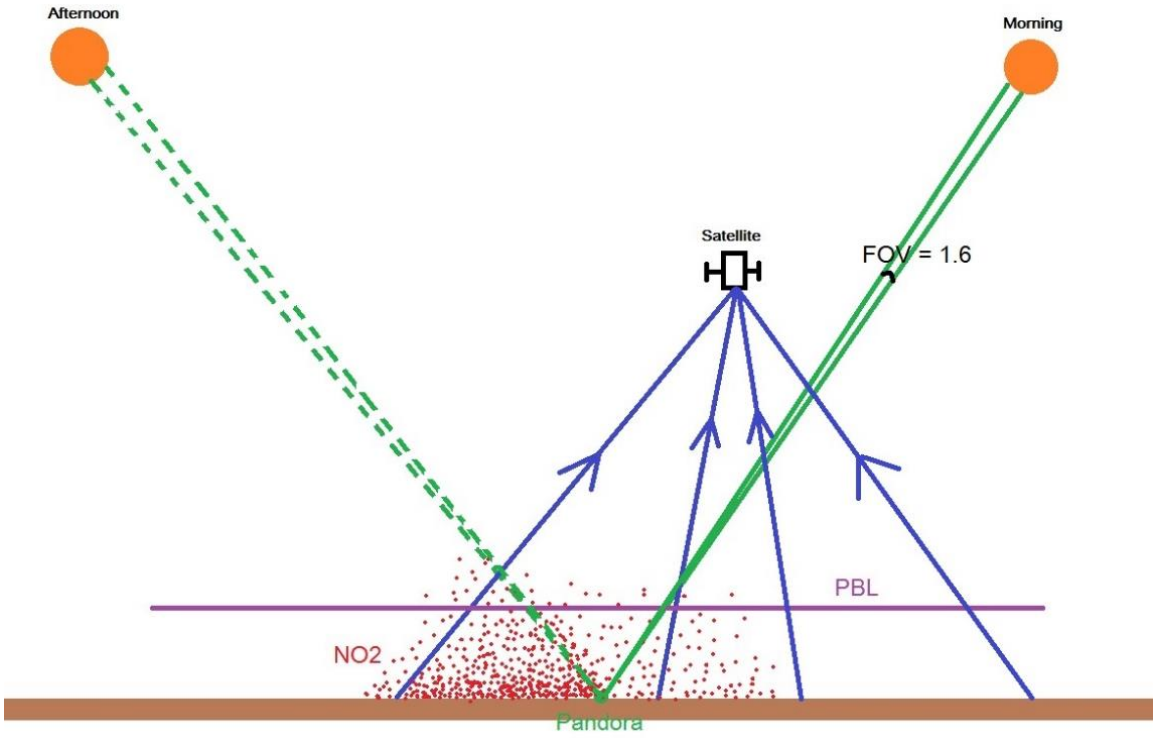

Figure S13. Schematic of remote and ground-based sensing of NO_2 VCDs. Green lines indicate the Pandora measurement rays, solid lines for the morning, and dash lines for the afternoon. Red dots denote NO_2 molecules. Blue lines represent the reflected radiation rays received by satellite. Orange circles denote the sun, and the purple line denotes the PBL height.

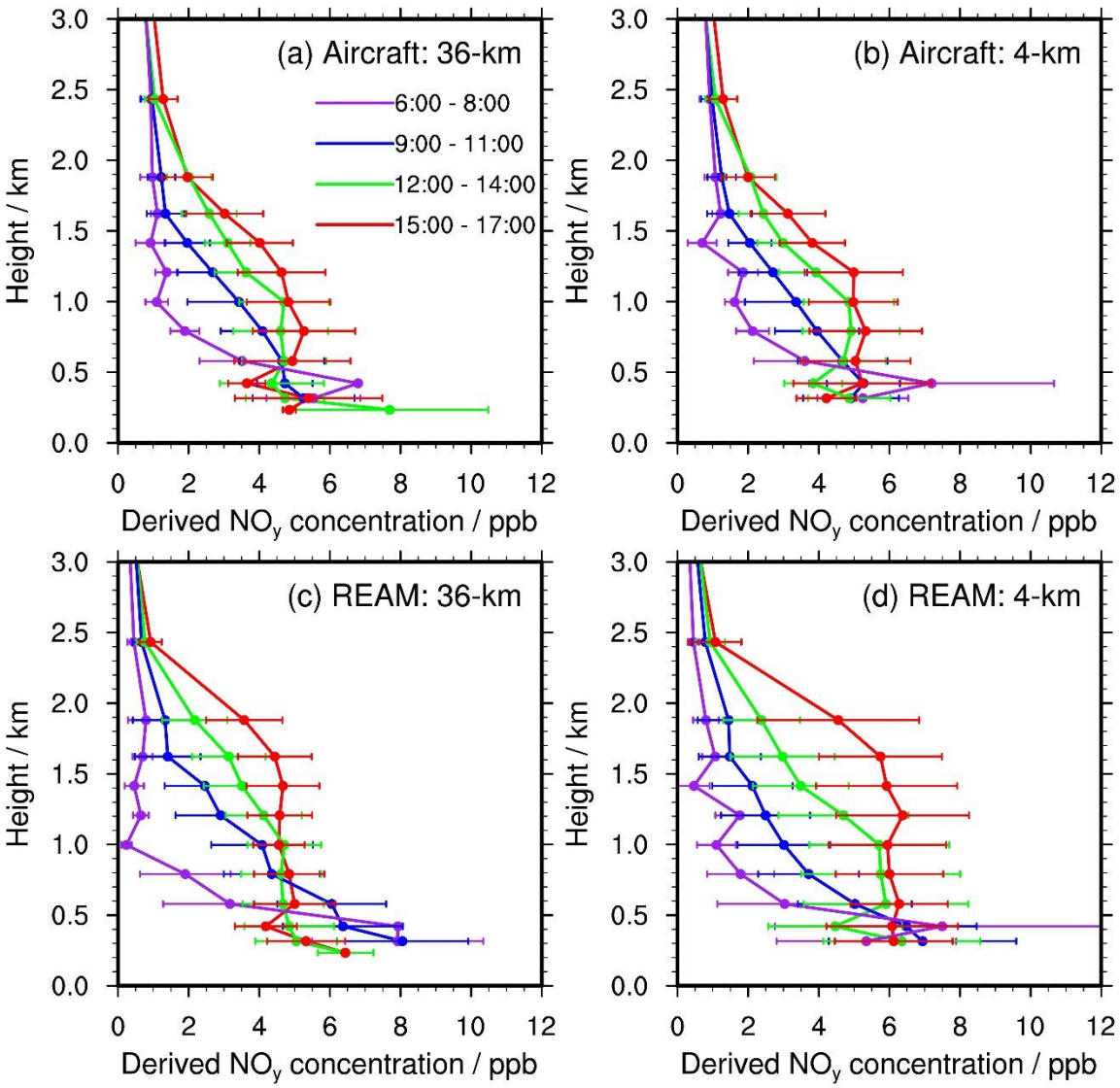

Figure S14. Temporal evolutions of derived-NO_y vertical profiles from the (a, b) P-3B aircraft and (c, d) REAM simulations at (a, c) 36-km and (b, d) 4-km resolutions during the DISCOVER-AQ campaign. Error bars denote the corresponding standard deviations. Due to the limited number of P-3B derived-NO_y observations and slightly different heights between 36- and 4-km grid cells from different WRF simulations (Table S2), small differences exist between the 36-km and 4-km observations when we bin them vertically to REAM grid cells (see also Table 1).

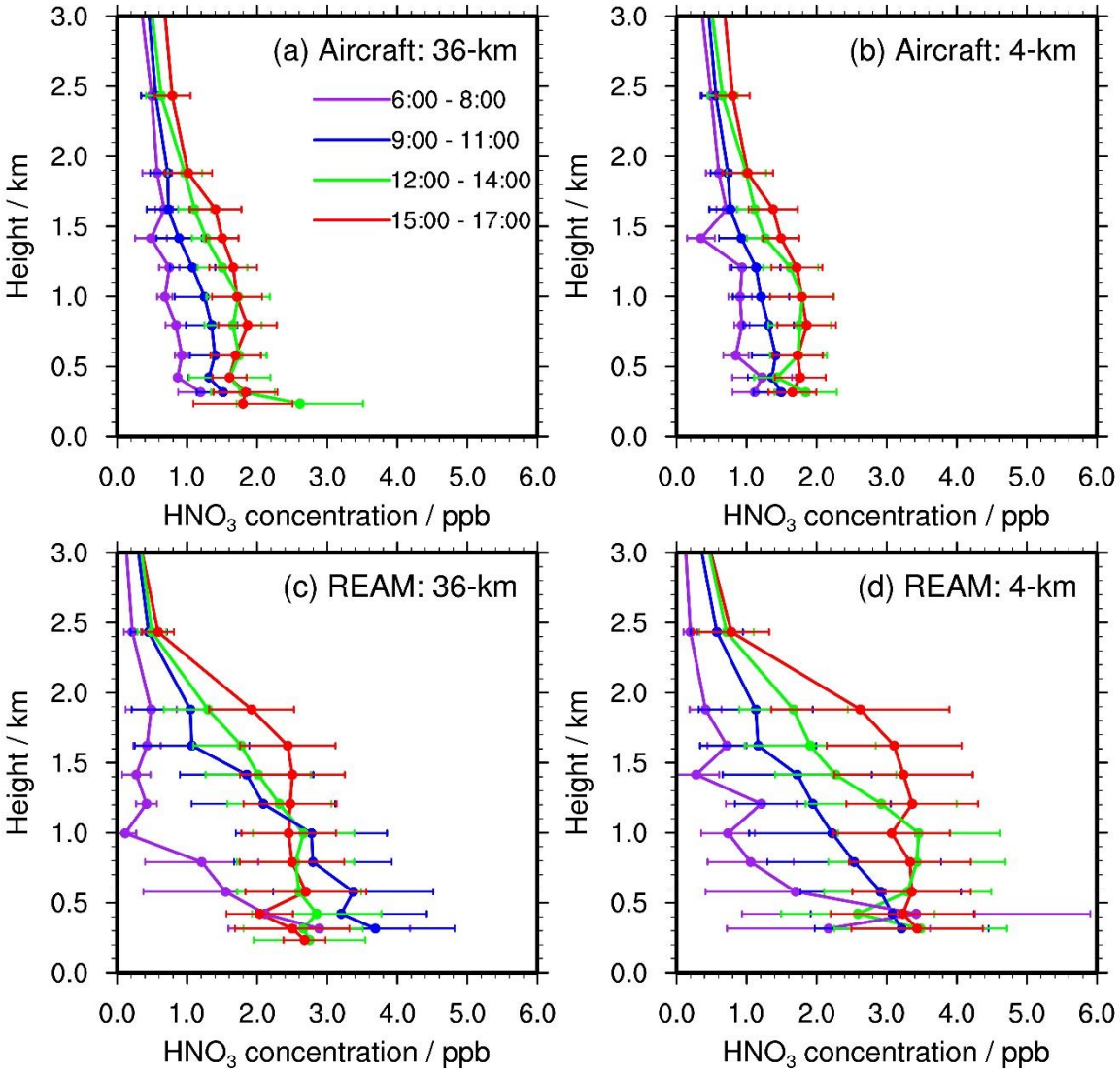

Figure S15. Same as Figure S14 but for coincident HNO_3 concentrations.

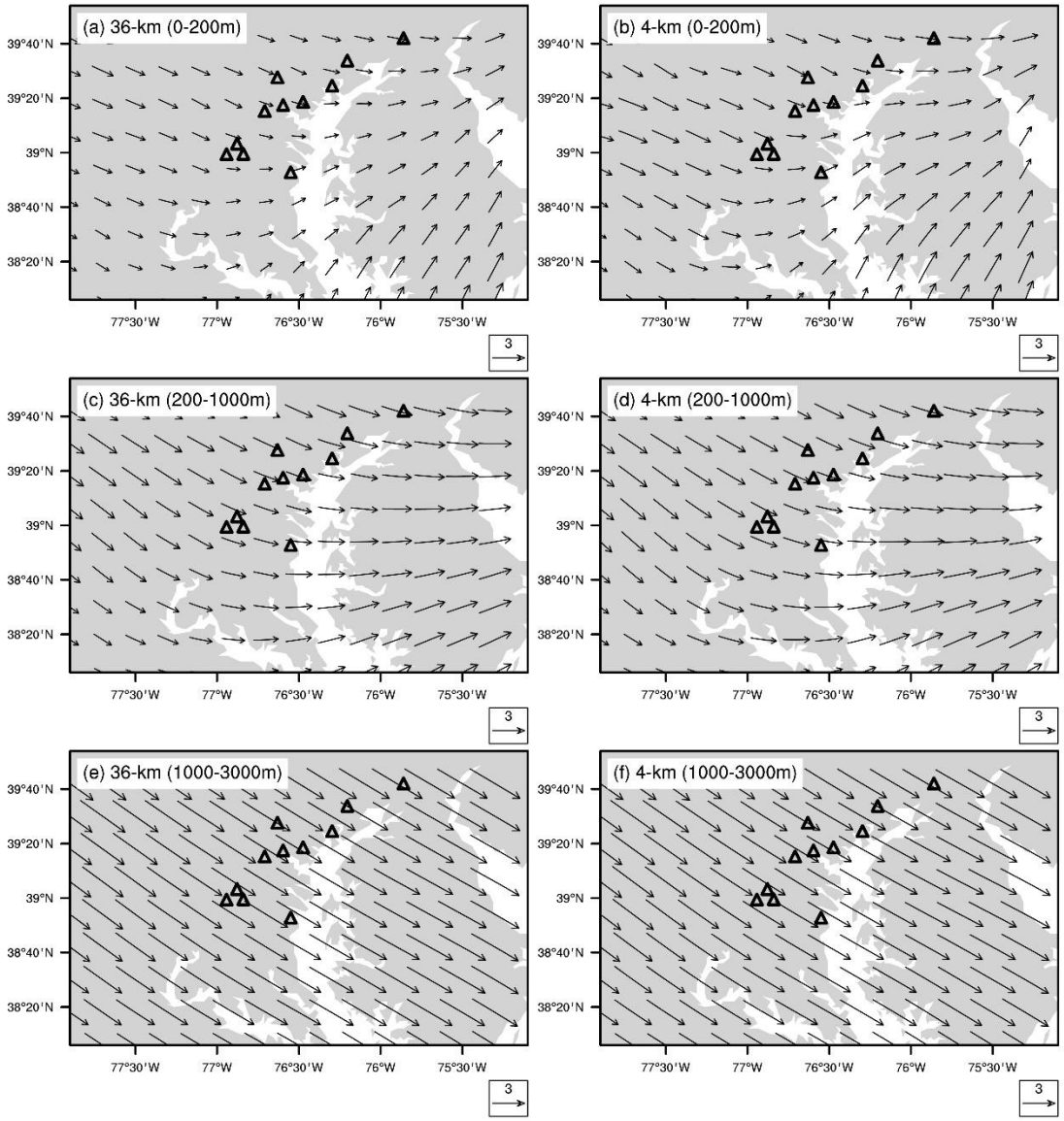

Figure S16. Comparisons of wind fields between the (a, c, e) 36-km and (b, d, f) nested 4-km WRF simulations for different height (AGL) bins in July 2011. (a) and (b) are for mean wind fields below about 200 m, (c) and (d) are for about 200 – 1000 m, and (e) and (f) are for about 1000 – 3000 m. Triangles denote the inland Pandora sites in Figure 1. The unit of wind speed is m s^{-1}.

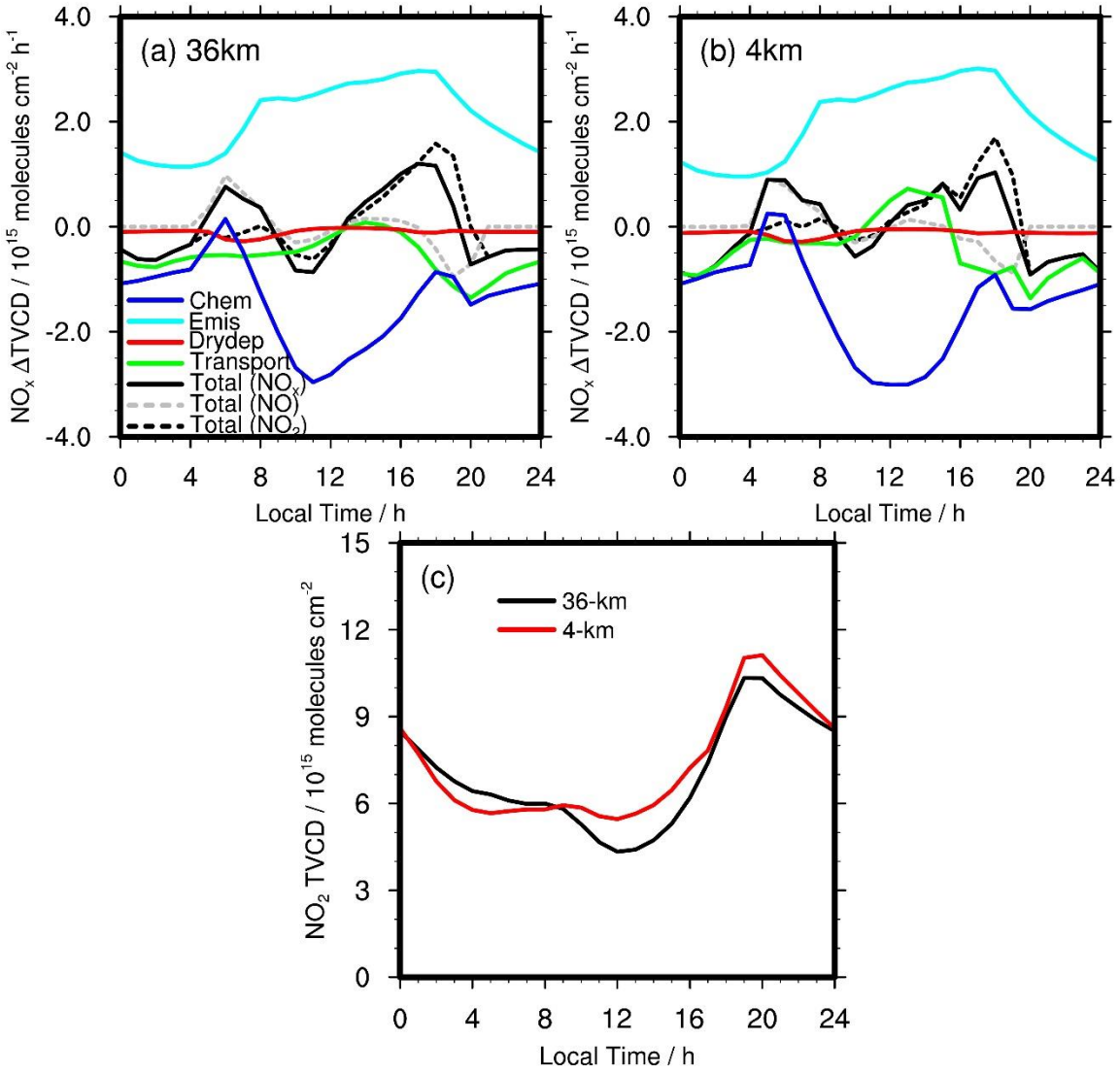

Figure S17. Contributions of emission, chemistry, transport, and dry deposition to NO_x TVCD diurnal variations over the six P-3B spiral sites (Figure 1 and Table S1) on weekdays in July 2011 for the (a) 36-km and (b) 4-km REAM simulations. "Chem" refers to net NO_x chemistry production; "Emis" refers to NO_x emissions; "Drydep" denotes NO_x dry depositions; "Transport" includes advection, turbulent mixing, lightning NO_x production, and wet deposition. "Total (NO_x)" is the hourly change of NO_x TVCDs ($\triangle(TVCD) = TVCD_{t+1} - TVCD_t$). "Total ($NO_2$)" is the hourly change of NO_2 TVCDs, and "Total (NO)" is the hourly change of NO TVCDs. (c), the 36-km and 4-km REAM simulated diurnal cycles of NO_2 TVCDs over the P-3B spiral sites on weekdays in July 2011. The black line in (c) denotes the 36-km REAM simulation results, and the red line denotes the 4-km REAM simulation results.

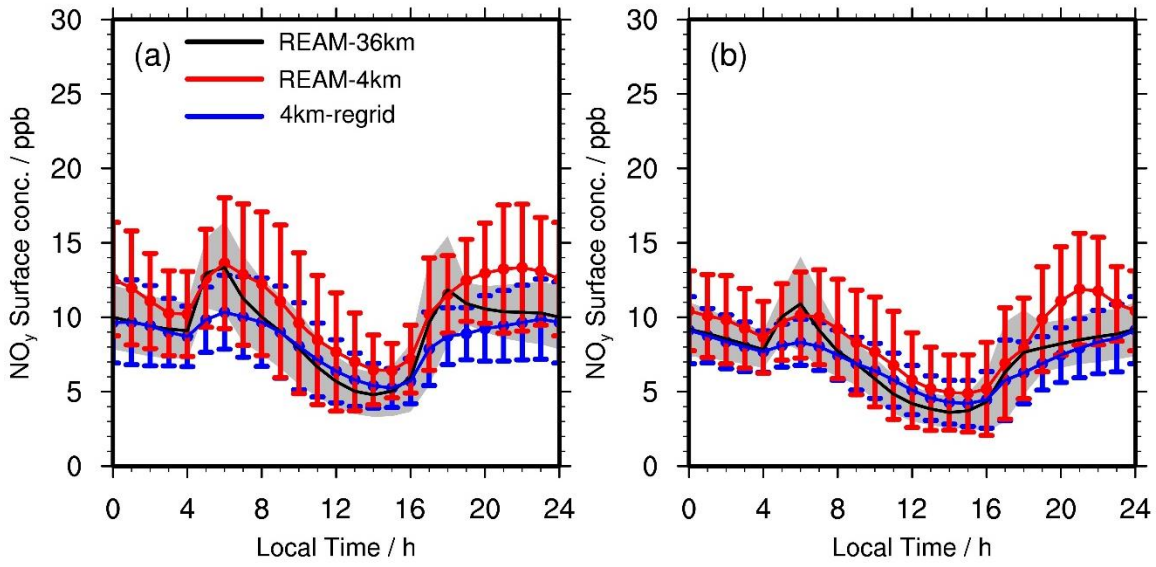

Figure S18. Comparisons of mean surface NO_y concentrations at Padonia, Edgewood, Beltsville, and Aldino between the 4-km and 36-km REAM simulations on (a) weekdays and (b) weekends for July 2011. "REAM-36km" (black lines) denotes the 36-km REAM simulation results; "REAM-4km" (red lines) denotes the 4-km REAM simulation results; "4km-regrid" refers to the 36-km values by re-gridding 4-km REAM simulation results into 36-km REAM grid cells. Error bars denote standard deviations.

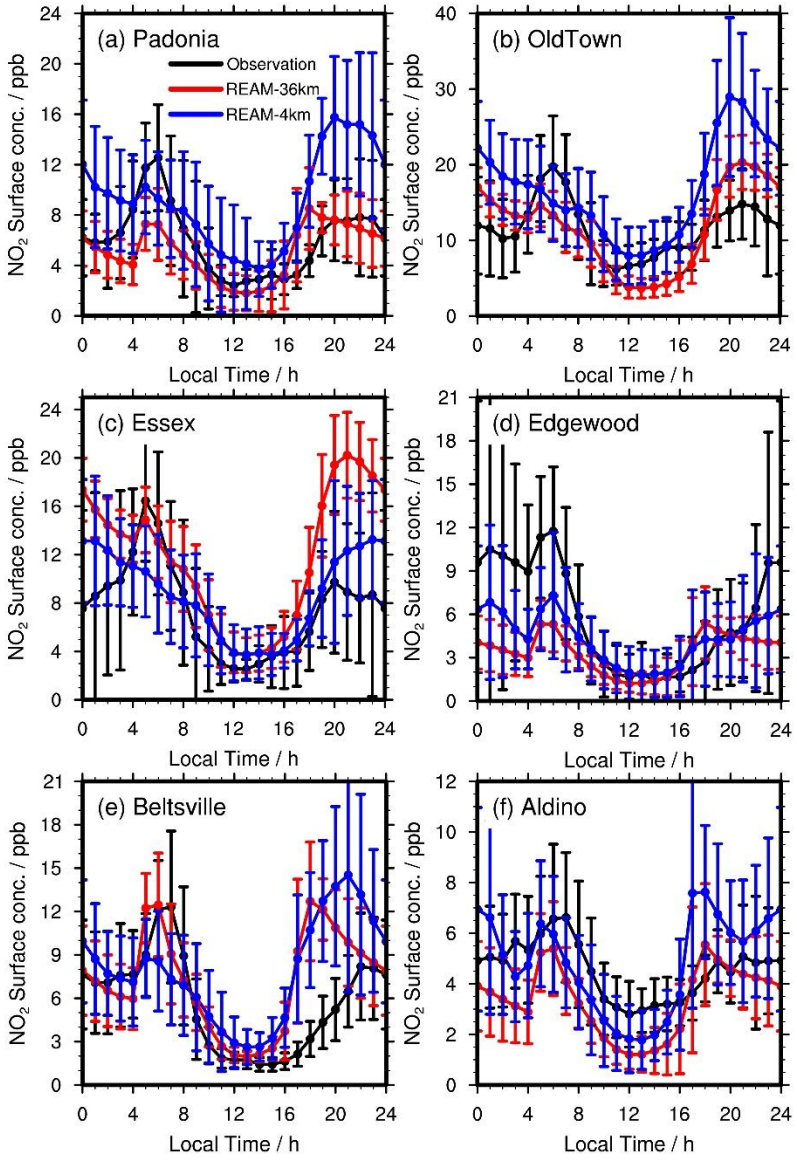

Figure S19. Same as Figure 7 but for individual observation sites on weekdays.

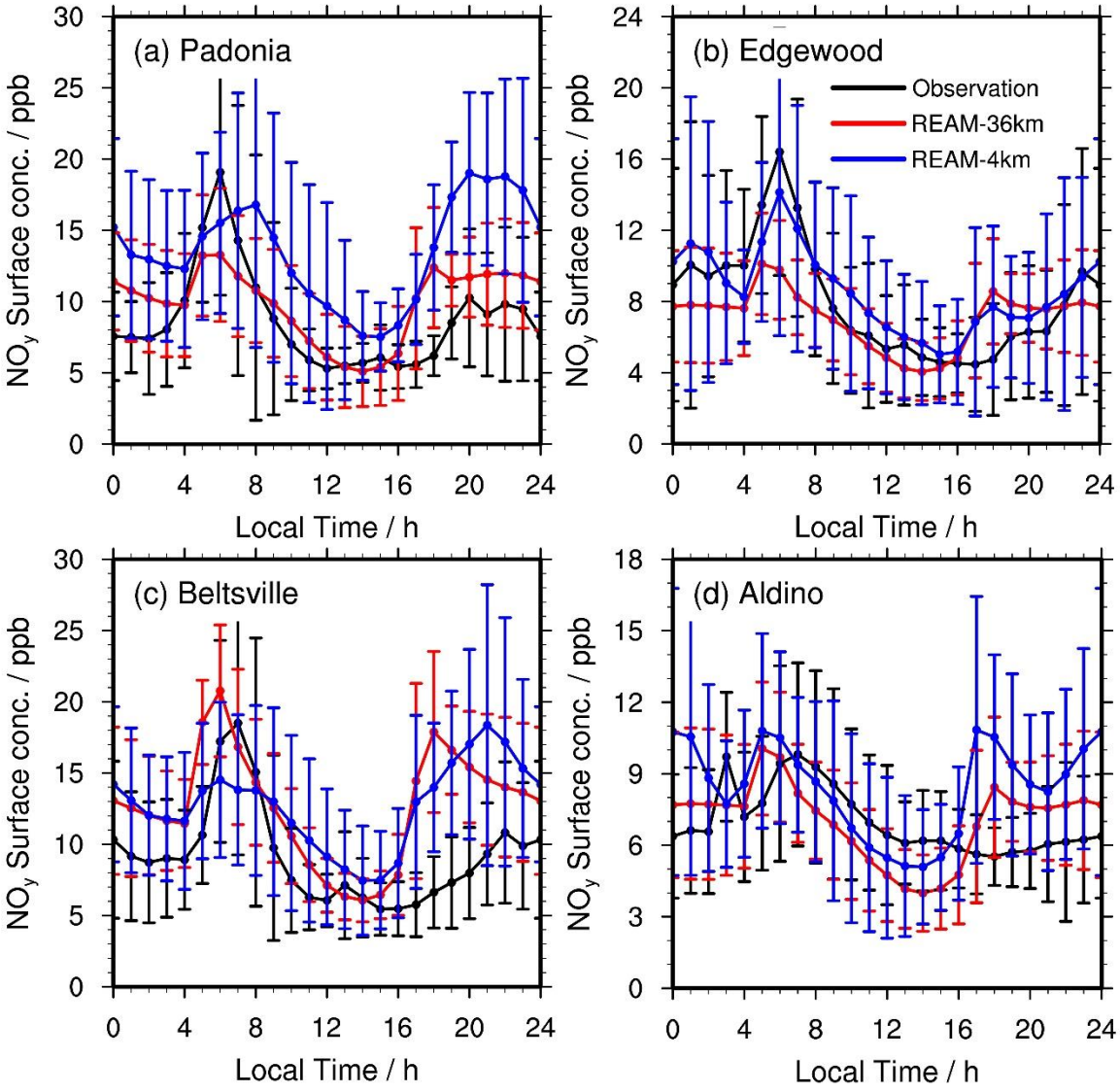

Figure S20. Same as Figure 12 but for individual observation sites on weekdays.

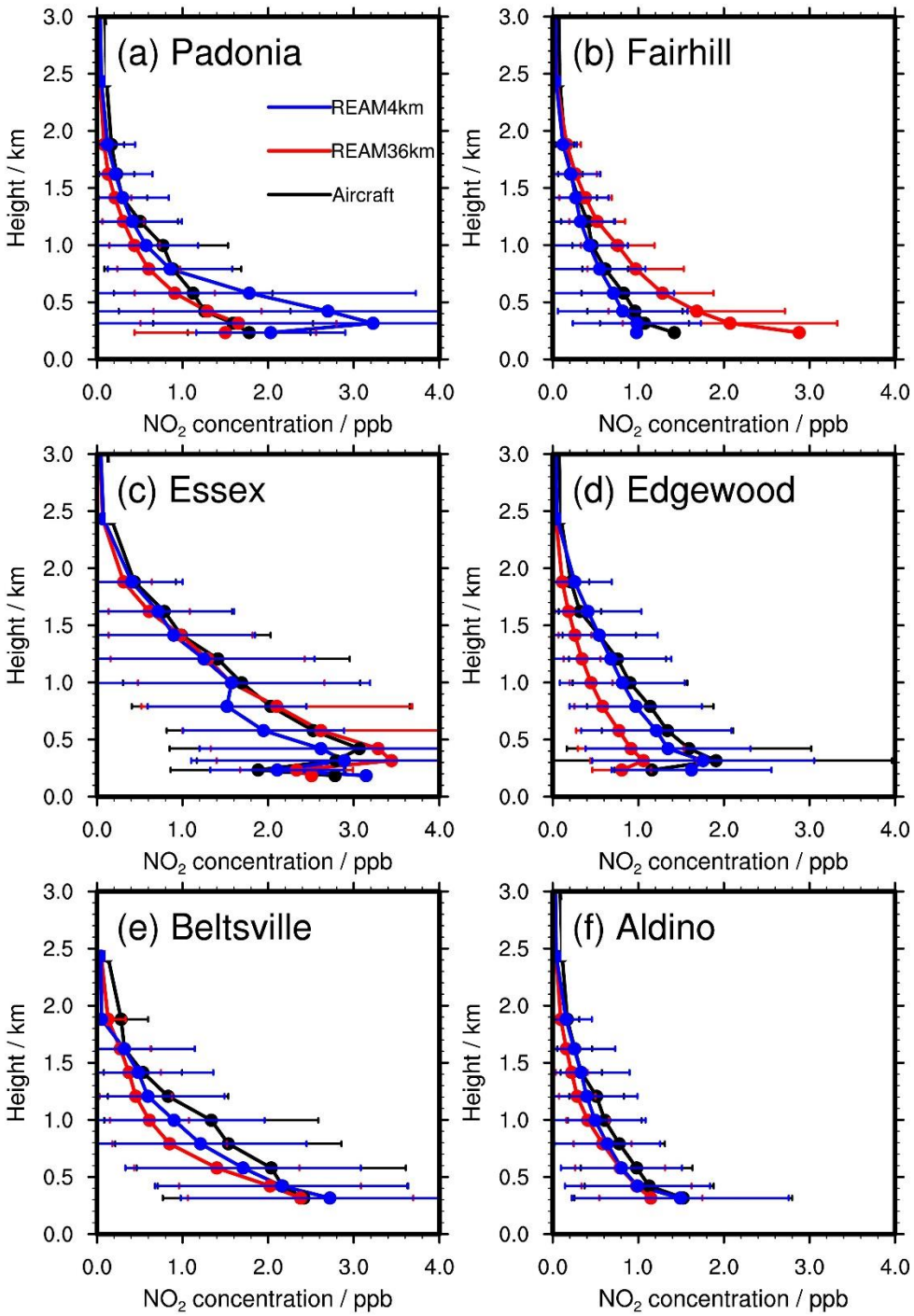

Figure S21. Comparison of NO_2 vertical profiles among P-3B aircraft observations and the 36-km and 4-km REAM simulations on weekdays in July 2011 for different spiral sites. Here we calculate the average of all available weekday NO_2 vertical profiles for each spiral site but do not consider the temporal evolutions shown in Figure 8.

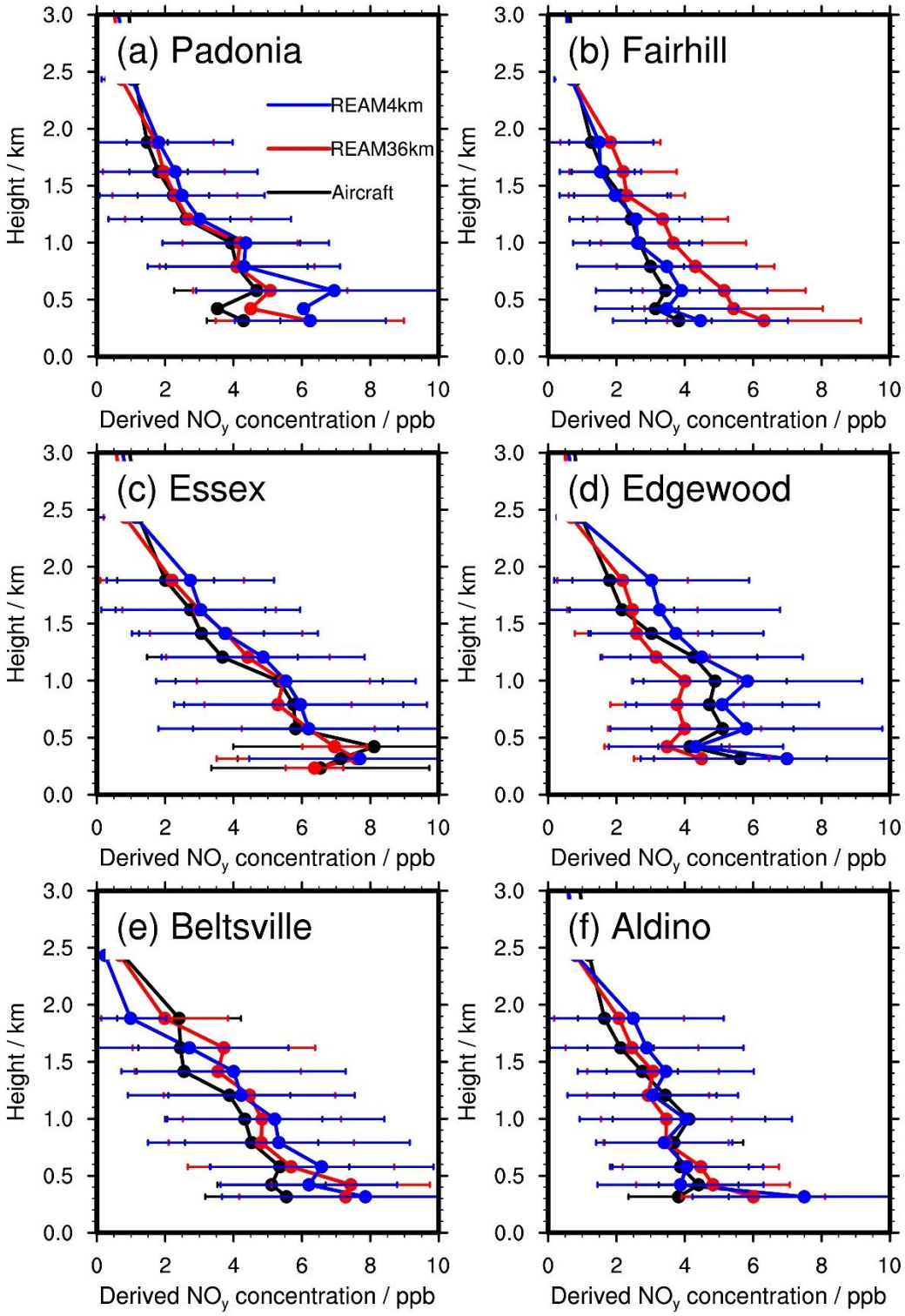

Figure S22. Same as Figure S21 but for derived-NO_y vertical profiles.

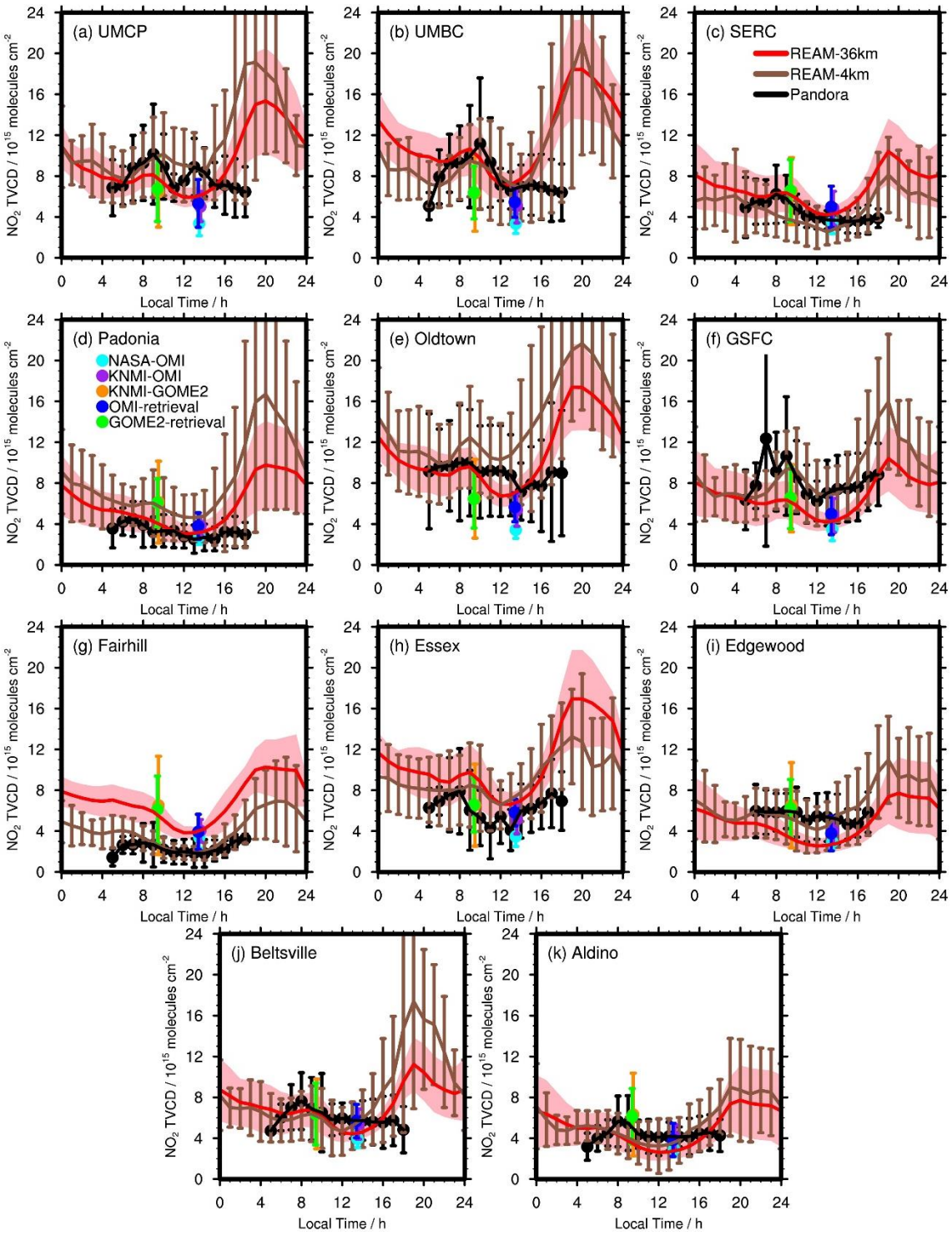

Figure S23. Same as Figure 10 but for individual Pandora sites on weekdays. Here we do not include P-3B aircraft-derived NO_2 VCDs below 3.63 km.

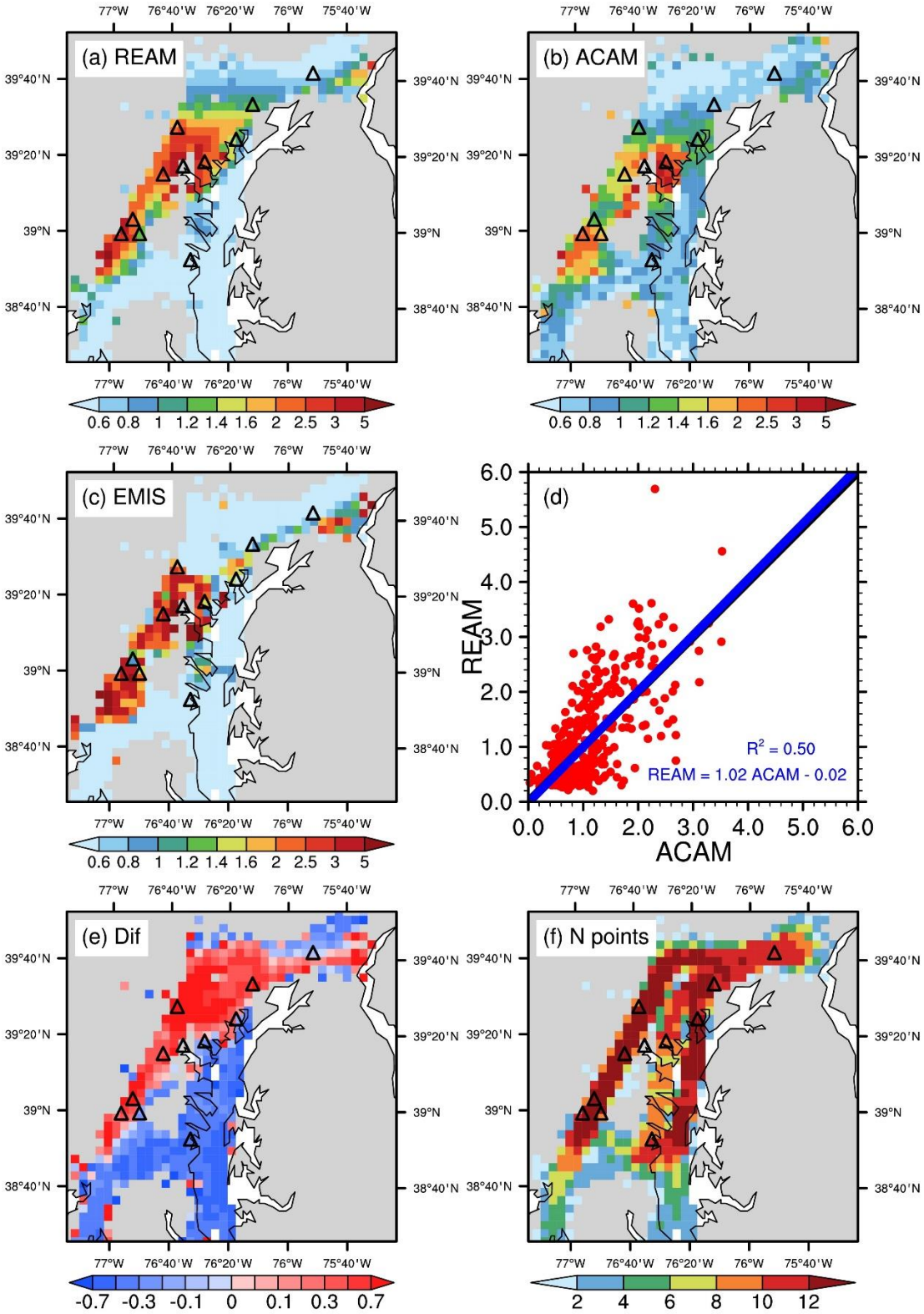

Figure S24. Same as Figure 14 but for weekends in July 2011. The domain averages of ACAM and coincident 4-km REAM NO_2 VCDs are 3.0 ± 1.7 and 3.3 ± 2.7 × 10^{15} molecules cm^{-2}, respectively.

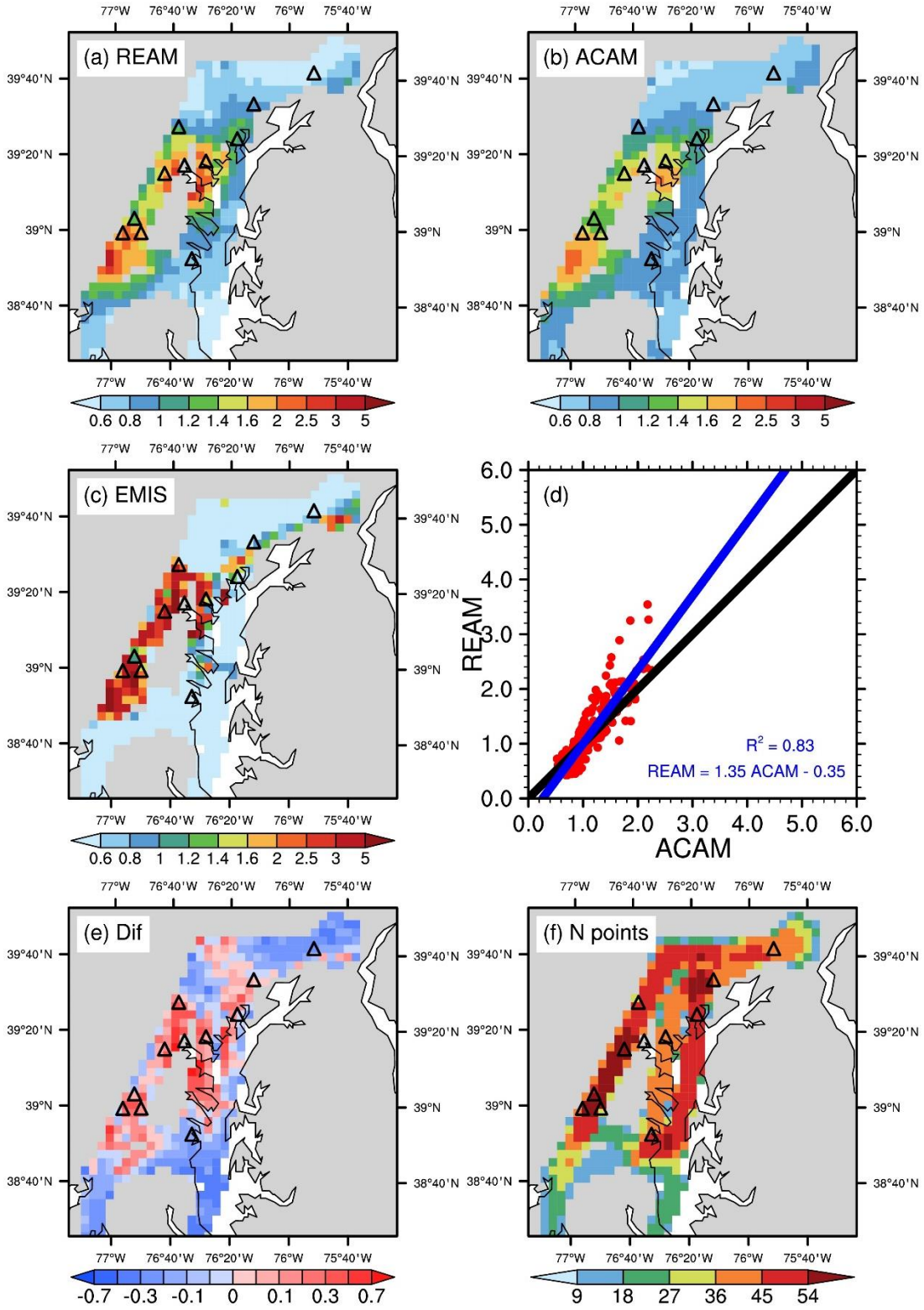

Figure S25. Same as Figure 14 but for grid cells with the number of data points ≥ 10, as shown in (f). The domain averages of ACAM and coincident 4-km REAM NO_2 VCDs are 5.3 ± 1.8 and 4.6 ± 2.4 × 10^{15} molecules cm^{-2}, respectively.

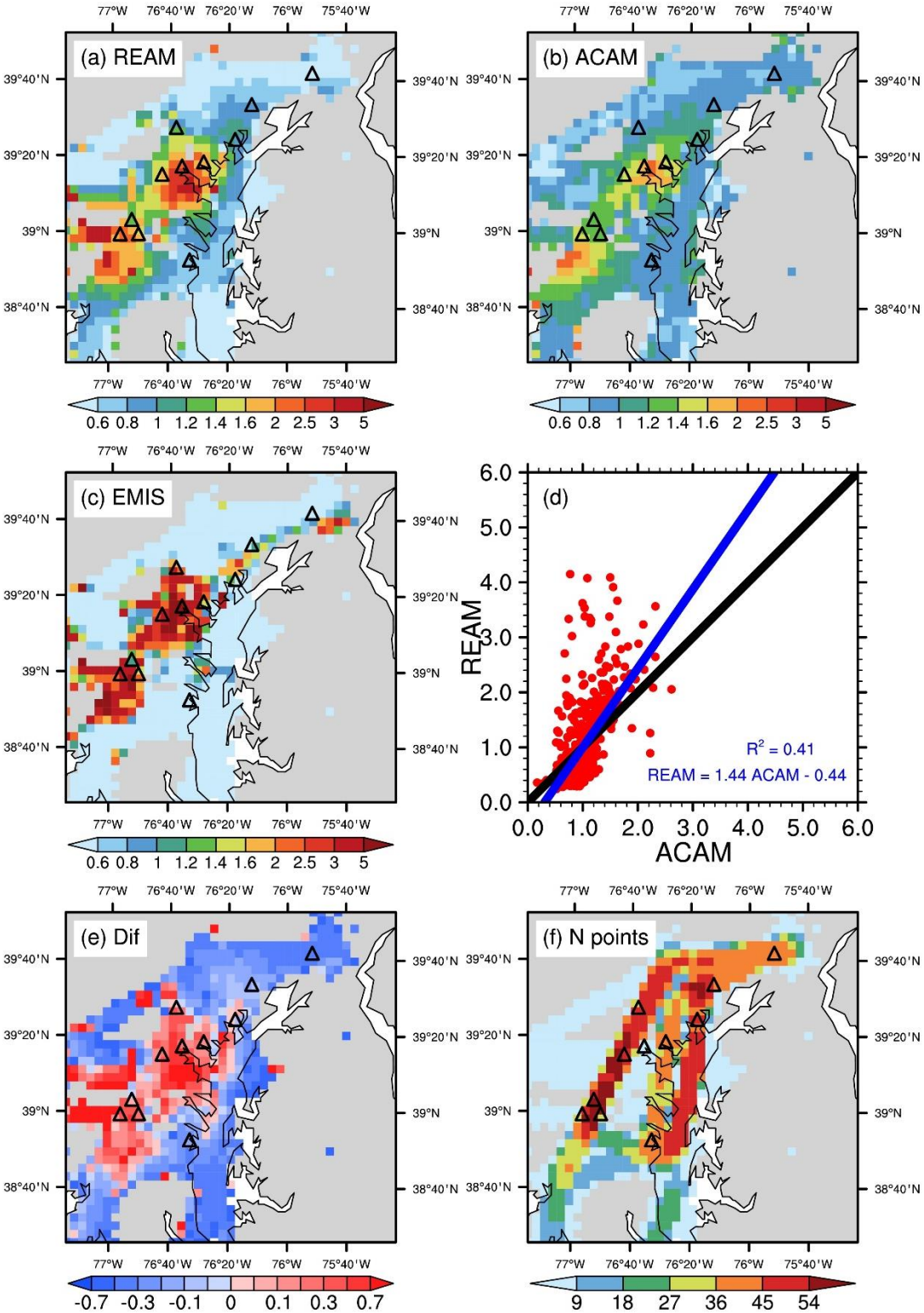

Figure S26. Same as Figure 14 but for weekday ACAM datasets obtained from https://www-air.larc.nasa.gov/cgi-bin/ArcView/discover-aq.dc-2011?UC12=1#LIU.XIONG/ (last access: December 31, 2019). The domain averages of ACAM and coincident 4-km REAM NO_2 VCDs are 5.9 ± 1.8 and 4.6 ± 3.1 × 10^{15} molecules cm^{-2}, respectively.

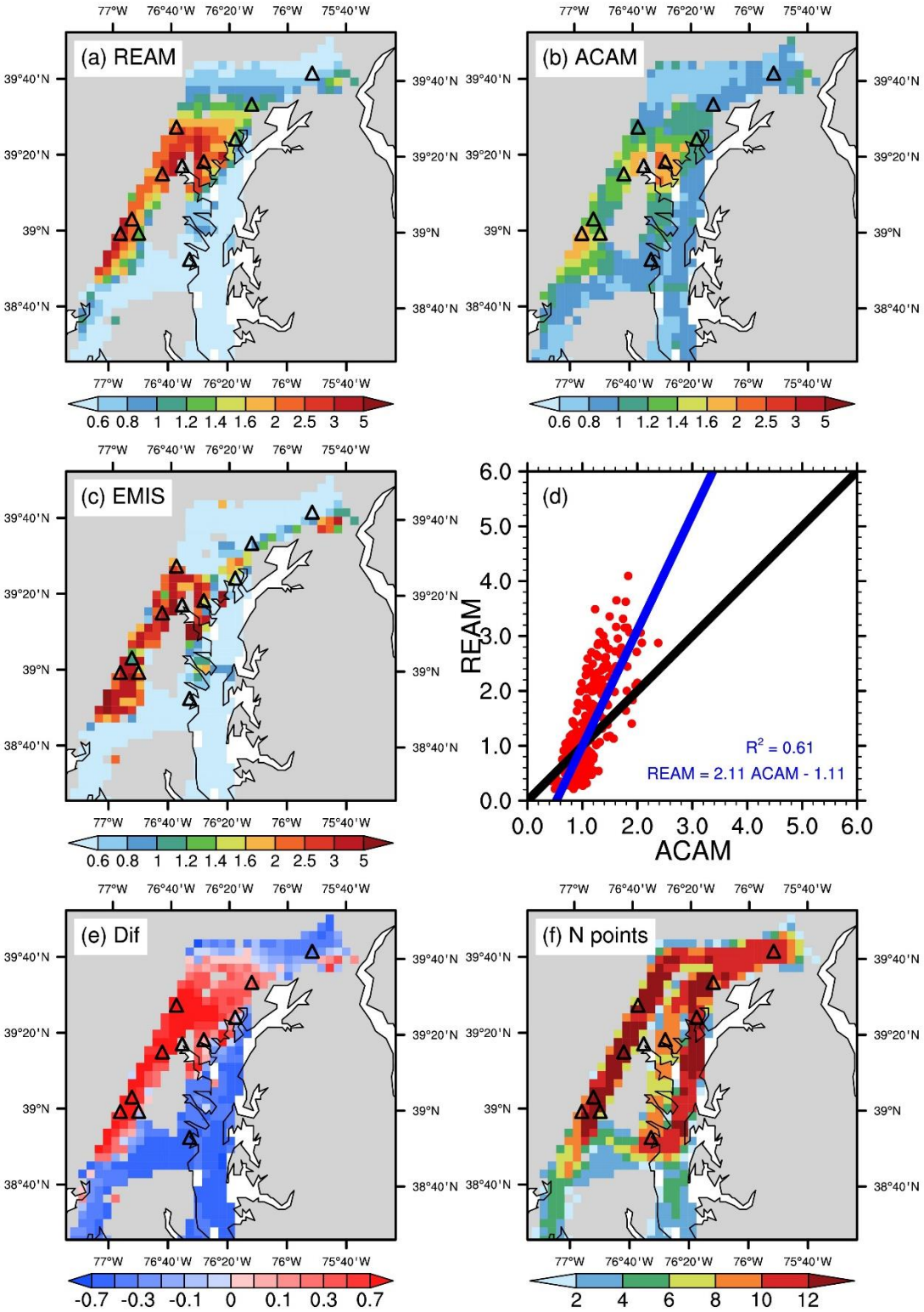

Figure S27. Same as Figure S26 but for weekend ACAM datasets obtained from https://www-air.larc.nasa.gov/cgi-bin/ArcView/discover-aq.dc-2011?UC12=1#LIU.XIONG/ (last access: December 31, 2019). The domain averages of ACAM and coincident 4-km REAM NO_2 VCDs are 4.7 ± 1.4 and 3.4 ± 2.7 × 10^{15} molecules cm^{-2}, respectively.

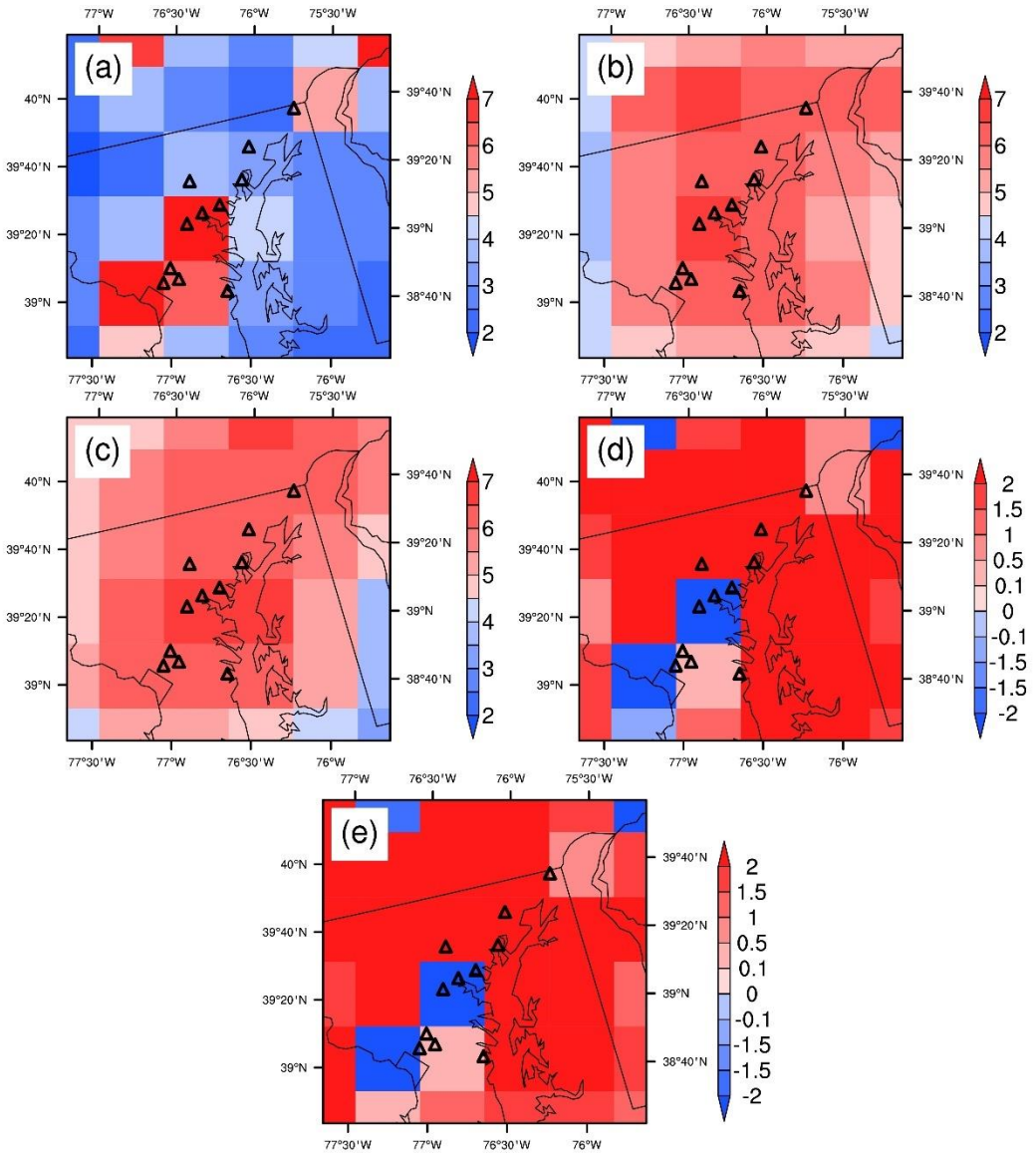

Figure S28. Distributions of weekday NO_2 TVCDs around the DISCOVER-AQ 2011 region for 9:30 LT in July 2011: (a) the 36-km REAM simulation results, (b) the KNMI GOME-2A product, (c) for the retrieved GOME-2A NO_2 TVCDs by using the KNMI DOMINO algorithm with corresponding 36-km REAM vertical profiles, (d) distribution of the NO_2 TVCD differences (b minus a) between KNMI GOME-2A and 36-km REAM, and (e) the difference (c minus a) between retrieved GOME-2A NO_2 TVCDs and the 36-km REAM results. The NO_2 TVCD unit is 10^{15} molecules cm^{-2}.